Jurnal Media Mesin, Vol. 27 No. 2
Printed ISSN: 1411-4348
Online ISSN: 2541-4577

EVALUATION OF CORROSION UNDER INSULATION AND REMAINING LIFE OF CARBON STEEL PIPELINES

Muhammad Syukron
Metallurgical Engineering Department
Universitas Pembangunan Nasional Veteran Yogyakarta, Indonesia
Email: muhammad.syukron@upnyk.ac.id

Dahniar
Metallurgical Engineering Department,
Universitas Pembangunan Nasional Veteran Yogyakarta, Indonesia
Email: 116210001@student.upnyk.ac.id

Muhammad Rizky Fajarullah
Metallurgical Engineering Department
Universitas Pembangunan Nasional Veteran Yogyakarta, Indonesia
Email: 116210002@student.upnyk.ac.id

Aura Wulanuari
Metallurgical Engineering Department
Universitas Pembangunan Nasional Veteran Yogyakarta, Indonesia
Email: 116210058@student.upnyk.ac.id

Kikin Hermanto
Technical Inspection
PT. Pupuk Kalimantan Timur
Email: kikin.hermanto@pupukkaltim.com

ABSTRAK

Analisis *Corrosion Under Insulation* (CUI) dan perhitungan umur sisa pipa material A-106-B akibat korosi dilakukan berdasarkan standar API 571 dan ASME B31.3 yang bertujuan untuk menegtahui parameter operasional dan lingkungan terhadap terbentuknya CUI pada pipa tersebut sehingga data dan analisa bisa digunakan untuk evaluasi dan tindakan yang diperlukan. Pengujian yang digunakan antara lain uji komposisi kimia menggunakan alat *Positive Material Identification type portable* OES dan XRF, pengujian ketebalan pipa menggunakan *Ultrasonic Thickness* dan mikroskop optik, pengujian deposit korosi pada pipa menggunakan SEM-EDX, dan pengujian kekerasan menggunakan alat *Micro Vickers Hardness Test*. Hasil analisis menunjukkan bahwa pipa tersebut mengalami korosi pada bagian *Outside Diameter* (OD) yang dikategorikan sebagai CUI. Produk korosi pada luar permukaan pipa yang terbentuk adalah Fe_2O_3 dan Fe_3O_4. Hasil dari nilai kekerasan pada spesimen dipengaruhi oleh lingkungan sekitar yang menyebabkan spesimen menjadi lebih keras. Perhitungan sisa umur pipa menunjukkan bahwa pipa NG memiliki sisa umur 2,0 tahun, pipa CG memiliki sisa umur 5,4 tahun dan pipa CH memiliki sisa umur 9,2 tahun.

Kata kunci: A-106-B, API 571, ASME B31.3, *Corrosion Under Insulation*, Pipa

ABSTRACT

Analysis of Corrosion Under Insulation (CUI) and calculation of the remaining life of corroded pipes of A-106-B material is carried out based on API 571, and ASME B31.3 standards which aim to determine the operational and environmental parameters for the formation of CUI on the pipeline. The tests used include chemical composition test using Positive Material Identification type portable OES and XRF, pipe

thickness testing using Ultrasonic Thickness and microscope, corrosion deposit on the pipes was tested using SEM-EDX, hardness testing using Micro Vickers Hardness Test. The results of the analysis showed that the pipe had corrosion in the Outside Diameter (OD) which was categorized as CUI. The corrosion products on the outside of the pipe surface that are formed are Fe_2O_3 and Fe_3O_4. The result of the hardness value in the specimen is influenced by the surrounding environment which causes the specimen to become harder. The calculations of the remaining life of the pipes are 2.0, 5.4 and 9.2 years for NG, CG and CH pipes respectively.

Keywords: *A-106-B, API 571, ASME B31.3, Corrosion Under Insulation, Pipe*

1. INTRODUCTION

The reliability of piping systems is essential for maintaining safe and continuous operation in ammonia and urea production plants. The primary function of a piping system is to distribute process feed and utility streams among plant units while transferring finished products to storage facilities or pipeline systems [1]. The insulated piping system is extensively used to transport process fluids under required operating conditions. In addition, The insulation reduce heat energy loss, improve process efficiency, increase personnel safety, and maintain operating conditions.

Despite the benefits of insulation, deterioration of the insulation system can create favorable conditions for corrosion under insulation (CUI). CUI is widely recognized as a dominant degradation mechanism for insulated piping in chemical and process industries because this corrosion is hidden behind the insulation layer, making it difficult to detect visually [2]. The consequences of CUI can be substantial, as demonstrated by an incident in 2006 in which a leak caused by CUI in an aging petrochemical plant triggered a fire that damaged approximately half of the processing unit. The incident resulted in economic losses of approximately USD 50 million and caused irreversible environmental damage [3].

CUI can affect various metallic materials used in insulated piping systems. In this study, particular attention is given to carbon steel piping, which is susceptible to external corrosion when moisture is retained beneath the insulation. Corrosion that occurs in insulated pipes begins with water entering or becoming trapped at a point where the insulation is damaged, causing the pipe to be imperfectly sealed. The trapped water is the main factor causing CUI. An illustration of CUI occurring in steel can be seen in Figure 1.

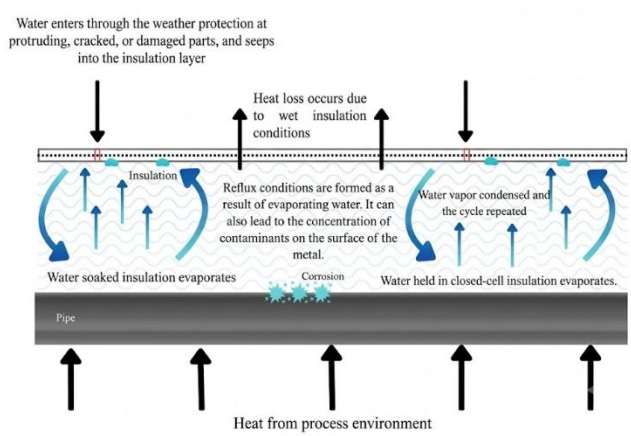

Figure 1. Illustration of the CUI mechanism

As illustrated in Figure 1, after water penetrates the insulation, it is absorbed or trapped. Once the water touches the hot steel surface, it evaporates. The evaporated water vapor then moves through the insulation toward the external barrier or cooler jacket, where condensation occurs. This condensed water then migrates back through the insulation toward the hot metal surface, and the process repeats.

Previous studies have investigated corrosion under insulation (CUI) from various perspectives. Geary [4] investigated a CUI-induced failure in an ASTM A106 Grade B carbon steel hydrocarbon line, showing that water ingress through damaged weatherproofing resulted in severe external corrosion and significant wall-thickness loss. The investigation combined chemical analysis, hardness testing, metallography, SEM-EDX, and thickness measurements to characterize the failed piping. The study provides valuable evidence of CUI-induced degradation. Yeow et al. [5] stated that corrosion under insulation (CUI) is a degradation mechanism that is difficult to detect at an early stage and is influenced by various factors, including operating temperature, insulation condition, coating quality, environmental conditions, and piping characteristics. Furthermore, variations in wall thickness and inspection history can affect the risk of failure, with greater wall loss resulting in a higher predicted probability of failure (PoF). Yang and Liu [6] investigated the corrosion behavior of carbon steel under insulation under different thermal and wet-dry conditions. Their results showed that cyclic temperature and wet-dry conditions accelerated CUI and increased the corrosion rate of carbon steel, with corrosion rates determined from mass loss measurements showing good agreement with electrochemical measurements. These findings demonstrate the significant influence of operating and moisture conditions on the progression of CUI and the resulting material degradation.

However, these studies have primarily addressed individual aspects of CUI, including failure characterization, environmental effects, corrosion-rate evaluation, and failure-risk assessment. Relatively limited attention has been given to an integrated assessment of actual CUI damage that combines wall-thickness measurements, material and corrosion-product characterization, corrosion-rate determination, minimum required thickness, and remaining life. Therefore, an integrated condition-based assessment is needed to evaluate the current integrity of CUI-affected piping and determine its remaining life.

2. METHOD

The samples tested were taken from pipes handling three different fluids. NG pipe handled natural gas, CG pipe handled coverted gas and CH pipe handled high pressurized condensate. The specifications of the samples tested can be seen in Table 1.

Table 1. Sample specifications

Spesification	NG Pipe	CG Pipe	CH Pipe
Diameter	½ inch	½ inch	½ inch
Fluid type	Natural Gas	Converted Gas	Washing Condensate High Pressure
Unit Section	Ammonia desulphurization, reforming & CO-Converter Section	Ammonia desulphurization, reforming & CO-Converter Section	Urea Synthesis and Decomposition Section
Line number	21	32	18
Material Class	A-106-B	A-106-B	A-106-B
Insulation Type	Personnel Protection	Personnel Protection	Hot Insulation
Design Temperature	-10˚ hingga 380˚C	-10˚ hingga 280˚C	150 ˚C
Operating Temperature	325˚C	226˚C	120 ˚C
Design Pressure	46.5 kg/cm^2	37.5 kg/cm^2	30 Kg/cm^2
Test pressure	90.7 kg/cm^2	61.39 kg/cm^2	45.27 Kg/cm^2
Insulation thickness	30 mm	25 mm	25 mm
Schedule	80	80	80
Pipe thickness	0.147 inch (3.73 mm)	0.147 inch (3.73 mm)	0.147 inch (3.73 mm)
Outer diameter	0.830 inch (21.3 mm)	0.840 inch (21.3 mm)	0.830 inch (21.3 mm)

In addition, one spare pipe sample in good condition was used for comparison with the corroded pipe. The spare sample material was A-106-B.

The method used was an experimental method involving six tests, namely visual testing, composition testing, thickness testing, metallographic testing, SEM testing, and hardness testing. Before conducting the tests, there were several standards that we used. For thickness testing using ultrasonics, the commonly used standard was ASTM E797 (Standard Practice for Measuring Thickness by Manual Ultrasonic Pulse- Echo Contact Method). The testing standards used in the preparation of metallographic test specimens are ASTM E3 (metallography) and ASTM E407-07 (etching). The testing standards and test specimens used in static hardness testing are ASTM E92 for Vickers testing.

The following are the testing procedures performed:

1. Visual Testing
   Visual analysis aims to determine whether the tested sample has undergone CUI (Corrosion Under Insulation). This visual analysis is based on the API 571 standard.
2. Composition Testing
   Composition testing on samples aims to determine the elements contained in the sample. This test is conducted to determine the type of material and standards suitable for use in testing. The tools used in composition testing are positive material identification type portable XRF and positive material identification type portable OES.
3. Thickness Testing
   Thickness measurements were carried out using an Ultrasonic Thickness Tester. The Ultrasonic Testing (UT) system consists of a transmitter and receiver circuit, a transducer, and a display unit[7]. Measurements were performed at ten longitudinal positions (points 1–10) along each specimen to obtain representative thickness data and determine the actual wall thickness. At each longitudinal position, thickness was measured at four circumferential orientations: 0˚, 90˚, 180˚, and 270˚. Prior to testing, each specimen was marked with a reference line designated as 0˚. During the measurements, the specimens were positioned with the reference mark facing upward. The circumferential measurement directions were defined as 0˚ (top), 90˚ (right), 180˚ (bottom), and 270˚ (left), and this orientation was maintained consistently for all specimens. The measurement locations are illustrated in Figure 2.

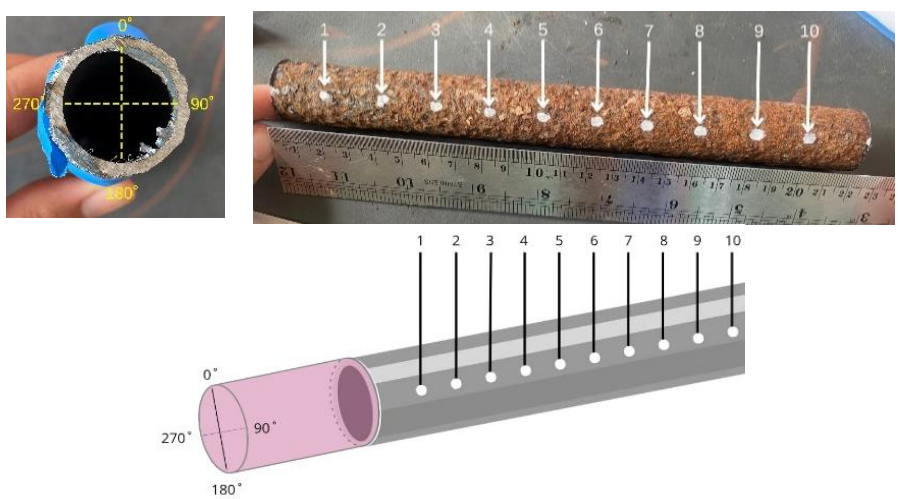

Figure 2. Sample measurement location

4. Metallographic Characterization

Metallography is the analysis of the microstructure and physical constituents of metals or alloys through direct visual observation or microscopic techniques, such as optical and electron microscopy[8]. The preparation of this microstructure itself aims to prepare the metal material so that it can be analyzed quantitatively and qualitatively. Before observing the microstructure with a microscope, sample preparation processes are required. The sample to be tested must be prepared through the specimen preparation stages. The following are the stages of microstructure preparation of a sample [9]:

a. Sampling
   Selecting the right sample from an object for microscopic study is very important. The selection of samples is based on the purpose of the observation to be carried out. Samples are taken from areas where the microstructure and macrostructure will be observed.
b. Cutting
   Cutting is the process of cutting the sample. The cutting must be precise and careful, because if not, it can cause the microstructure to change or be damaged. During the cutting process, friction inevitably occurs between two metals, namely between the metal to be cut and the cutting tool (saw). Therefore, during cutting, care must be taken to prevent friction that can generate excessive heat and damage the microstructure, thus requiring coolants. Coolants are cooling fluids.
c. Mounting
   Basically, the samples being tested are very small or have irregular shapes, making them very difficult to handle for the next preparation processes, namely grinding and polishing. Therefore, to make it easier for us to hold the test objects, the samples must be mounted.
d. Grinding
   Grinding is one of the specimen preparation stages, in which sanding is carried out to level and smooth the surface of the specimen. Sanding is carried out using sandpaper of various sizes, which are indicated by mesh size. Sanding is carried out starting from a low mesh number (coarse) to a high mesh number (fine). During the sanding process, water coolants are applied. Water serves to minimize damage caused by heat, which can alter the microstructure of the sample and extend the life of the sandpaper. Sanding flattens and smoothes the surface of the sample by rubbing it against abrasive paper/sandpaper.
e. Polishing
   Polishing is the final process in specimen preparation to obtain a smooth workpiece surface by applying alumina to the sample surface to achieve a smooth and shiny sample surface.
f. Etching
   Etching is a metallographic process used to selectively reveal microstructural features by chemically attacking the polished surface of a metal specimen. In this study, the specimens were etched using Nital, a solution consisting of nitric acid (HNO_3) and 95% ethanol, to reveal the microstructural features of the specimens.
g. Microscope Examination
   After the etching process, the specimens were examined using an Olympus GX53 optical metallurgical microscope at a magnification of 5x, 10x, 20×, 50x, and 100x to observe the microstructure and measure the actual wall thickness of the corroded pipes. The observed microstructures were then analyzed to identify ferrite and pearlite phases as well as corrosion-induced wall thinning.

5. SEM Testing
   Scanning Electron Microscope (SEM) testing is a microscopic analysis method that uses electron beams to produce images of the sample surface. Thus, SEM testing is a very useful tool in various fields of research and industry, especially for observing the structure and composition of sample

surfaces with high resolution. In Addition, SEM–EDX testing was conducted to identify the elemental composition of corrosion deposits formed on the outer surface of the corroded A106-B pipes. The analysis focused on determining the major elements contained in the corrosion products, such as Fe, O, and C, in order to identify the corrosion products associated with Corrosion Under Insulation (CUI).

6. Hardness Testing
   Hardness testing is carried out using a Micro Vickers Hardness Tester. Hardness testing is carried out by indenting 9 points, where 3 points represent the OD (Outside Diameter) area, 3 points represent the center area, and 3 points represent the ID (Inside Diameter) area. The following are the test areas on the sample, which can be seen in Figure 3

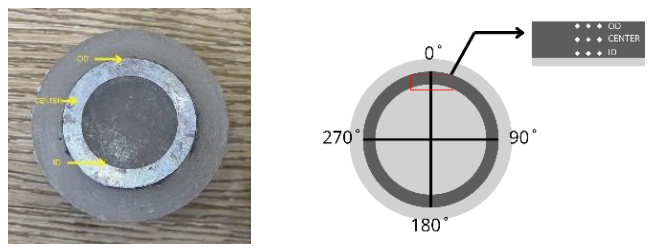

Figure 3. Hardness testing areas

The overall research flow is shown in Figure 4.

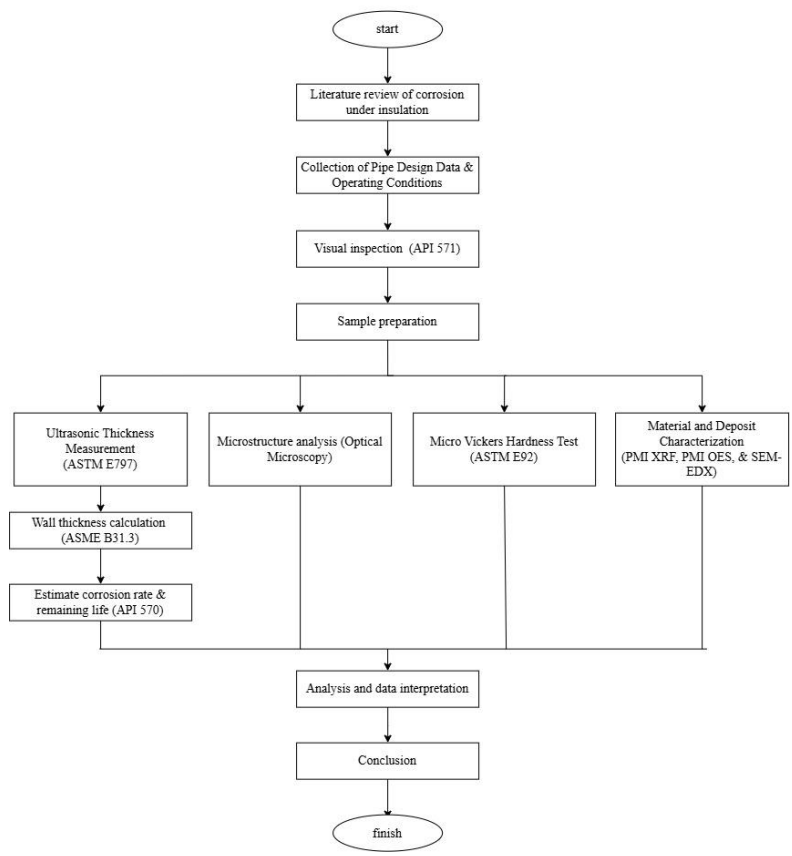

Figure 4. Research flow diagram

3. RESULTS AND DISCUSSION

3.1 *Pipe Corrosion Conditions*

Visual observation of the analyzed pipes based on API 571 standard showed that each pipe had *corrosion under insulation* (CUI) with uneven and peeling surface conditions, rough appearance, unprotected rust, holes, and loose crust covering. The pipe surface conditions are shown in Figure 5.

Figure 5. Pipe surface conditions (a) NG (b) CG (c) CH

3.2 *Comparative Analysis of Specimen Composition*

Based on the results of composition testing using Positive Material Identification type portable OES and Positive Material Identification type portable XRF, the elemental content (%) of the A-106-B pipe specimen is presented in Table 2.

Table 2. Comparison of corroded pipe composition test results with ASTM A-106-B standard composition

Element	PMI XRF Test Results Composition (%)			PMI OES Test Results Composition (%)			ASTM A106 Grade B Standard Composition (%)
	NG	CG	CH	NG	CG	CH	
Fe	99.16	98.42	98.35	99.7	98.3	98.3	97.04-97.81
C	-	-	-	0.209	0.148	0.148	0.3 (max)
Mn	0.43	0.74	0.76	0.404	0.757	0.757	0.29-1.06
P	-	-	-	0.0159	0.0164	0.0164	0.035 (max)
S	-	-	-	0.0045	0.0047	0.0047	0.035 (max)
Si	0.23	0.26	0.29	0.191	0.205	0.205	0.1 (min)
Cr	-	0.03		0.0245	0.0813	0.0813	0.4 (max)
Cu	0.04	0.32	0.31	0.4	0.294	0.294	0.4 (max)
Mo	-	0.04	0.03	0.005	0.0356	0.0356	0.15 (max)
Ni	-	0.08	0.11	0.0068	0.117	0.117	0.40 (max)
V	0.04	0.03	0.06	0.004	0.0012	0.0012	0.08 (max)

The results of the PMI OES and PMI XRF composition tests show significant percentage values, except that some elements were not detected by the PMI XRF device. This is because the PMI XRF testing device has limitations in identifying low elemental content such as carbon (C), sulfur (S), boron (B), nitrogen (N), and others. The chemical composition test results of pipes that have undergone corrosion show that they are still within the ASTM A106 Grade B standard composition range, indicating that the age of the pipes and the corrosion process do not alter the chemical composition of the pipes.

3.3 *Comparison of Specimen Thickness Values with Spare Specimens*

The thickness of NG, CG, and CH pipes measured with an ultrasonic tester is presented in Table 3.

Table 3. Comparison of UT thickness test results for corroded pipes and spare pipes

Pipe Circumference Angle	Thinnest Thickness of NG Pipe (mm)	Thinnest Thickness of CG Pipe (mm)	Thinnest Thickness of CH Pipe (mm)	Spare Pipe Thickness (mm)
0˚	2.07	3.02	2.26	3.96
90˚	2.02	3.02	1.94	
180˚	2.04	3.05	2.30	
270˚	2.12	3.05	2.34	

The thickness of NG, CG, and CH pipes at each test angle produced lower thickness values than the spare pipe thickness. This can occur because when the pipe corrodes, oxidation of iron (Fe) to Fe^{2+} occurs, which then reacts with oxygen and water to form rust in the form of Fe_2O_3 or Fe_3O_4. The rust then forms on the area of the pipe that acts as a cathode, while the area that acts as an anode experiences a reduction in thickness. This can be clarified in the table with microstructure testing, where the wall thickness of the corrosion specimen is analyzed using the results of the microstructure. The thinnest thickness in the NG pipe specimen was found at the 90˚ angle, measuring 2.02 mm. In the CG pipe specimen, the thinnest thickness was found at the 0˚ angle, measuring 3.02 mm, while the thinnest thickness in the CH pipe specimen was found at the 0˚ angle, measuring 1.94 mm. The section with the thinnest thickness from the Ultrasonic Thickness was further observed using a microscope to determine the actual thickness of the pipe specimen. The results of thickness measurements using a microscope can be observed in Figure 6.

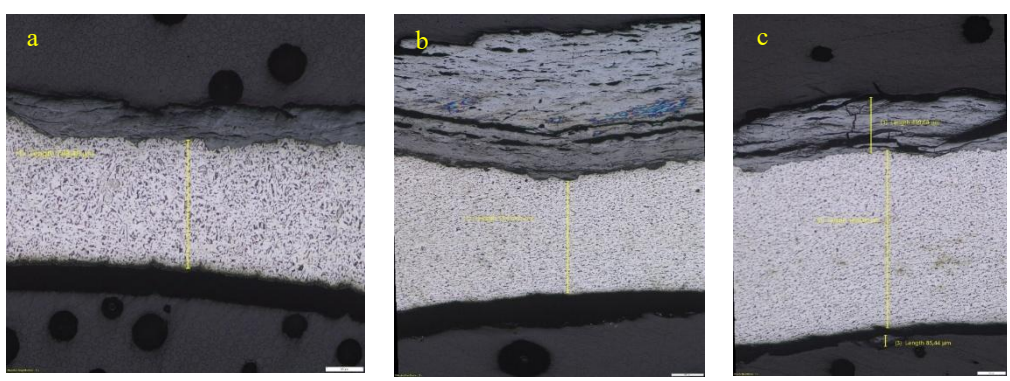

Figure 6. Pipe thickness using a microscope (a) NG (b) CG (c) CH

Measurements using microstructure results are more accurate because ultrasonic thickness (UT) testing detects deposits as pipe wall thickness and cannot test areas with corrosion-induced gaps (depressions) that are difficult to detect and test using UT equipment. The thicknesses obtained using a microscope on NG pipes, CG pipes, and CH pipes are 0.71 mm, 1.02336 mm, and 1.42 mm, respectively.

Both the UT analysis results and the microstructure analysis results indicate that the A-106-B pipe has experienced surface thinning due to corrosion, which has caused material loss on the pipe, and the prolonged exposure of the pipe has been in use is also a contributing factor.

3.4 *Comparison of Microstructures of Corroded Specimens with Spare Specimens*

The comparison of microstructures between spare pipe samples, NG, CG, and CH is presented in Figure 7.

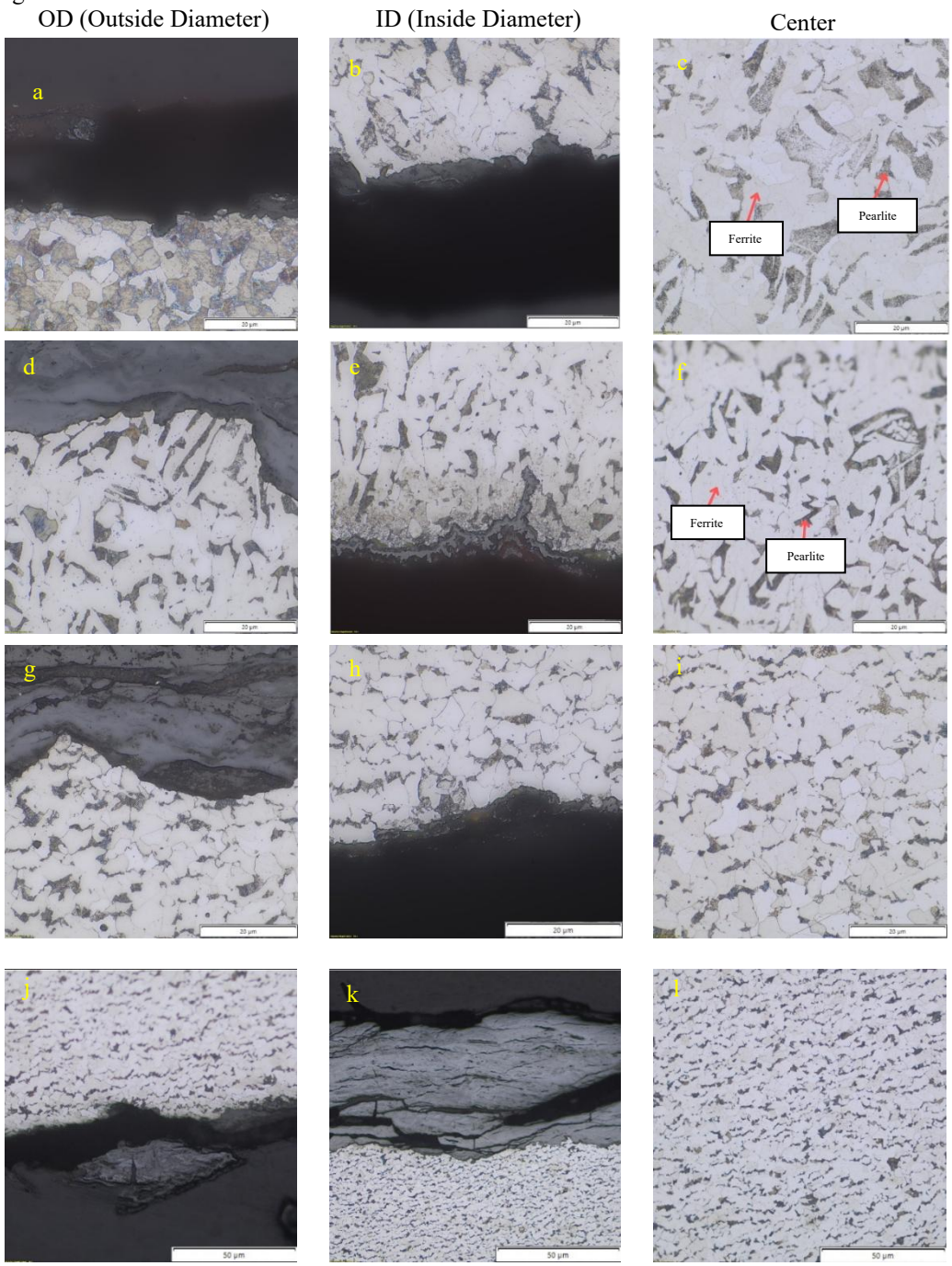

Figure 7. Microstructure of Pipe: (a-c) Spare; (d-f) NG; (g-i) CG; (j-l) CH

In the metallographic test results on the A106-B pipe specimen and the spare specimen, there are dark and light areas, indicating that the dark areas are pearlite phases, while the light areas are ferrite phases. The identification of ferrite and pearlite is consistent with previous metallographic observations of low-carbon steel, in which ferrite and pearlite were observed as the principal microstructural constituents [10]. The ferrite phase affects the material with soft and good magnetic properties in metals, while the pearlite phase affects the material with hard and strong properties. It can be seen that the CH specimen and the CG specimen with the spare specimen do not have significant microstructural results. In the Fe_3C diagram, the phase formed in low carbon steel is 0.148% with ferrite and pearlite phases in the CH specimen and 0.158% in the CG specimen. For the NG sample, the OD of the sample pipe was corroded and had corrosion products on the pipe surface. This could have occurred due to humid environmental conditions, which triggered oxidation and reduction reactions, resulting in rust products adhering to the pipe surface. In addition, there were also corrosion products on the ID, which were likely caused by the flow of pipe fluid. The fluid flowing through the pipe is the outlet from the hydrogenerator, namely sulfur compounds (H_2S). The corrosion that is likely to occur on the ID section is sulfidation corrosion. This type of corrosion is caused by H_2S gas that forms salt vapor, and is also supported by high temperatures, around 230˚C.

3.5 *Phase Percentage Analysis*

After obtaining the microstructure results, the phase percentage content of specimen A-106-B can be determined using a 20x magnification microscope. The following are the phase percentage calculations from the corrosion specimen, spare specimen, and lever rule calculations, as shown in Table 4.

Table 4. Comparison of phase percentage between corroded pipe and spare pipe

Specimen	Phase	Content (%)		
		NG	CG	CH
Corrosion Specimen	Ferrite	81.63	84,83	82,69
	Pearlite	17.88	14,82	16,77
Spare Specimen	Ferrite	81.82	81,82	81,82
	Pearlite	17,29	17,29	17,29
Lever Rule	Ferrite	74,66	81,57	82,93
	Pearlite	25,34	18,43	17,07

The table above shows that there is no significant difference in the comparison of ferrite and pearlite phase percentages in corrosion specimens, spare specimens, and level rule calculations. The phase percentage itself can affect the mechanical properties of a material, such as strength, ductility, and hardness.

3.6 *Analysis of Corrosion Product*

To identify chemical composition of deposits or corrosion products found inside and outside the A106-B pipes, SEM-EDX testings were conducted as represented in Table 5 and shown in Figure 8.

Table 5. Composition of Corroded Pipe Deposits

Element	*Atomic Conc.*			*Weight Conc.*		
	NG	CG	CH	NG	CG	CH
C	0.392	26.408	21.000	0.200	16.517	8.709
O	80.571	63.071	44.934	54.800	52.553	24.825
Si	0.167	0.205	0.413	0.200	0.300	0.400
Cr	0.000	0.000	2.230	0.000	0.000	4.004
Fe	18.870	10.015	30.365	44.800	29.129	58.559
Mo	0.000	0.300	1.057	0.000	1.502	3.504

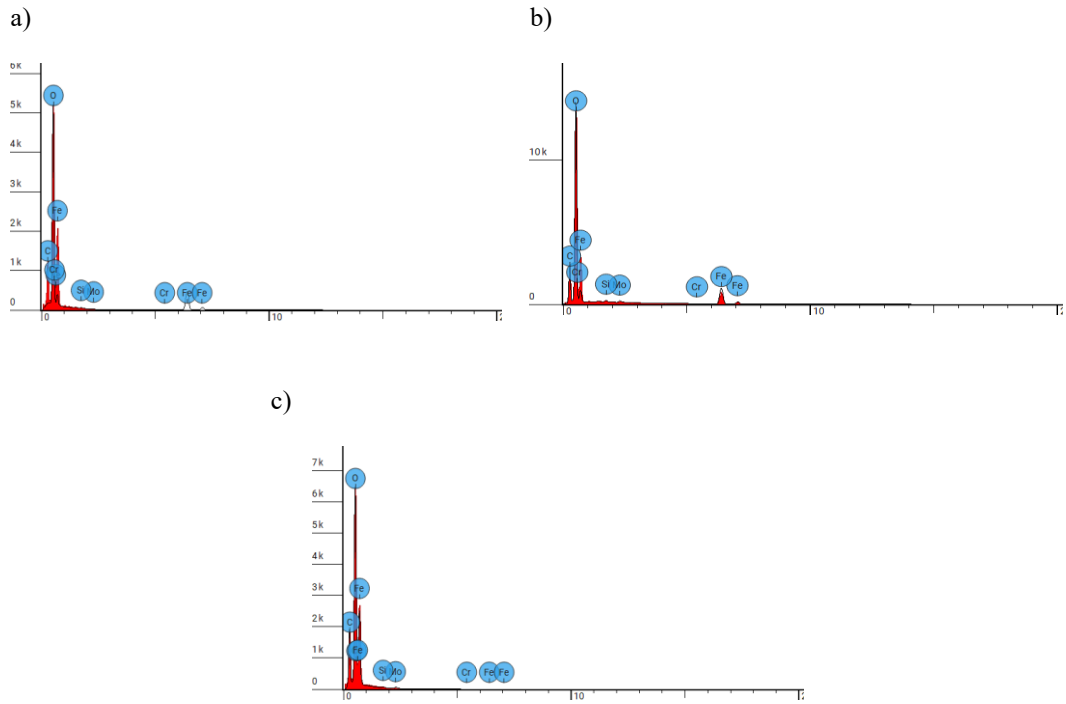

Figure 8. SEM-EDX analysis of corroded pipes: (a) NG; (b) CG; (c) CH

Based on the SEM-EDX test results taken from the outer diameter of the pipe (OD), the deposit results on the A-106-B pipe show that the three main elements with the highest percentages are iron (Fe), carbon (C), and oxygen (O). The presence of a fairly high oxygen content of 44.934%wt in the corrosion product indicates the oxidation of iron, which forms iron oxide products such as Fe_2O_3 or Fe_3O_4. Exposure of insulated A-106-B pipes to water will increase the rate of corrosion because water can be trapped in the pipe insulation, making it difficult to dry and causing increased moisture in the pipe. Water that has reacted with oxygen will form OH^- ions which, when reacting with Fe^{2+} or $Fe^{3+,}$ will form $Fe(OH)_2$ or $Fe(OH)_3$. When it dries or settles on the pipe, it will form Fe_2O_3 or Fe_3O_4 as corrosion products. The presence of carbon (C) from contaminants attached to the deposits is thought to originate from the grinding process during metallographic testing.

3.7 Comparison of specimen hardness values with spare specimens

The comparison of hardness values between spare pipe samples, NG, CG, and CH is presented in Table 6.

Table 6. Comparison of hardness values of corroded pipe specimens, spare pipe specimens, and ASTM A-106-B standard

Region	NG Pipe (HV)	CG Pipe (HV)	CH Pipe (HV)	Spare Pipe (HV)	Minimum Hardness Standard ASTM A-106-B(HV)
OD (Outside Diameter)	221	147.3	133.67	143	126.4
ID (Inside Diameter)	210	149.3	130.67	134.3	
Center	211,33	148.3	134.67	134.3	

Based on the Vickers hardness values obtained from laboratory tests, when compared to the minimum Vickers hardness standard with a minimum tensile strength of 60,000 Psi (415 MPa) or equivalent to 126.4 HV in ASTM A-106-B. In carbon steel, the Vickers hardness value can range from 120 to 180 HV. With the minimum tensile strength, the CH specimen and spare specimen remain within or above the minimum tensile strength value, indicating that the specimen material has resistance to maximum stress before undergoing deformation or structural damage.

3.8 *Minimum Required Thickness*

The Minimum Required Thickness is calculated to determine the minimum pipe thickness that can still be used. The Minimum Required Thickness calculation can be calculated based on the ASME B31.3 standard using Equations 1 and 2.

$$Tm = t + c \quad (1)$$

$$t = \frac{PD}{2\,(SEW+PY)} \quad (2)$$

Notation:
Tm = Minimum thickness required, including mechanical allowance, corrosion, and erosion
C = Total mechanical allowance plus corrosion and erosion *allowances*..
t = Pipe thickness
P = Pipe design pressure
D = Pipe outer diameter as listed in the standard table or specifications or as measured
S = Pipe allowable stress
E = Quality factor
W = Joint strength
Y = Temperature coefficient

The calculation of minimum required thickness of the pipe samples as follow,

- NG Pipe

Data:
P = 46,5 kg/cm^2 = 4,56 MPa (pressure design)
D = 0,840 in = 21,336 mm (schedule table)
S : 16,7 ksi = 115,14 MPa (Table A-1 ASME B31.3)
W : 1 (Table 302.3.5 ASME B31.3)
E : 1 (Table A-1B ASME B31.3)

Y : 0,4 (Table 304.1.1 ASME B31.3)
C : 0 Inch (Corrosion Allowance)
Calculation:

$$t = \frac{4.56\ MPa \times\ 21.336\ mm}{2\ (115.14\ \times 1\ \times 1 + 4.56\ \times 0.4)}$$

$$t = 0{,}4159 \text{ mm}$$

Tm = t + c

= 0,4159 + 0

= 0,4159 mm

- CG Pipe

Data:
P : 37,5 Kg/cm^2 = 3,677494 MPa (pressure design)
D : 0,840 inch = 21,336 mm
S : 18,28 ksi = 126,03616 MPa (Table A-1 ASME B31.3)
W : 1 (Table 302.3.5 ASME B31.3)
E : 1 (Table A-1B ASME B31.3)
Y : 0,4 (Table 304.1.1 ASME B31.3)
C : 0 Inch (Corrosion Allowance)
Calculation:

$$t = \frac{3.677494\ \times\ 21.336}{2\ (126.036161\ \times\ 1\ \times\ 1 + 3.677494\ \times\ 0.4)}$$

$$t\ = 0.30768\ mm$$

tm = t + c
= 0.30768 mm + 0 mm
= 0.30768 mm

- CH Pipe

Data:
P : 30 Kg/cm^2 = 2,942 MPa (pressure design)
D : 0,840 Inch = 21,336 mm
S : 20 Ksi = 137,895 MPa (Table A-1 ASME B31.3)
W : 1 (Table 302.3.5 ASME B31.3)
E : 1 (Table A-1B ASME B31.3)
Y : 0,4 (Table 304.1.1 ASME B31.3)
C : 0 Inch (Corrosion Allowance)
Calculation:

$$t = \frac{2.942\ \times\ 21.336}{2\ (137.895\ \times\ 1\ \times\ 1) + (2.942\ \times 0.4)}$$

= 0.45 mm

tm = t + c
= 0.45 mm + 0 mm
= 0.45 mm

After performing the calculation, it was found that the minimum required thickness for line number ½”-NG-01221-PC1-P6 is 0.4159 mm, line number ½” CG-1232-MB1S-P4 is 0.30768 mm, and line number ½” CH-02218-MB1-H2 is 0.45 mm.

3.9 *Remaining Life*

In assessing the remaining life of equipment affected by corrosion, the corrosion rate is a key parameter in the calculation. The corrosion rate can be determined in accordance with API 570 using Equation (3).

$$\mathrm{CR} = \frac{t\ initial - t\ actual}{time\ between\ t\ initial\ and\ t\ actual\ (year)} \tag{3}$$

Notation:
CR = Corrosion Rate (mm/year)
t initial = initial thickness at the start of use (mm)
t actual = Actual thickness at the end of use (mm)

The results of the corrosion rate calculation for the corroded pipe sample are as follows:

- NG Pipe

$$\mathrm{CR} = \frac{3.96\ \mathrm{mm} - 0.71\ \mathrm{mm}}{24\ \mathrm{years}}$$

$$\mathrm{CR} = 0.147\ \mathrm{mm/year}$$

- CG Pipe

$$\mathrm{CR} = \frac{3.96\ \mathrm{mm} - 1.02336\ \mathrm{mm}}{22\ \mathrm{years}}$$

$$\mathrm{CR} = 0.1335\ \mathrm{mm/year}$$

- CH Pipe

$$\mathrm{CR} = \frac{3.96\ \mathrm{mm} - 1.42\ \mathrm{mm}}{24\ \mathrm{years}}$$

$$\mathrm{CR} = 0.1058\ \mathrm{mm/year}$$

The remaining life of the pipe can be determined using Equation 4.

$$\mathrm{RSL} = \frac{\mathrm{Tac} - \mathrm{Tm}}{\mathrm{CR}} \tag{4}$$

Notation:
LT = Remaining Lifetime (years)
Tac = Thickness Actual (mm)
Tm = Thickness Minimum (mm)
CR = Corrosion Rate (mm/year)

The calculation of the remaining life of the corroded pipe are as follows:

- NG Pipe

$$\mathrm{RSL} = \frac{0.71\ \mathrm{mm} - 0.4156\ \mathrm{mm}}{0.147\ \mathrm{mm/year}}$$

$$\mathrm{LT} = 2.0\ \mathrm{years}$$

- CG Pipe

$$\mathrm{RSL} = \frac{0.30768\ \mathrm{mm} - 0.30768\ \mathrm{mm}}{0.1335\ \mathrm{mm/year}}$$

$$\mathrm{RSL} = 5.4\ \mathrm{years}$$

- CH Pipe

$$\text{RSL} = \frac{1.42\ \text{mm} - 0.45\ \text{mm}}{0.1058\ \text{mm/year}}$$

$$\text{RSL} = 9.2\ \text{years}$$

Based on these calculations, the remaining service life of the pipe with line number ½”-NG-01221-PC1-P6 is 2.0 years, line number ½” CG-1232-MB1S-P4 is 5.4 years, and line number ½” CH-02218-MB1-H2 is 9.2 years.

4. CONCLUSION

Based on the visual inspection, metallographic observation, hardness testing, and SEM–EDX analysis of the three piping samples (NG, CG, and CH), the corrosion mechanism was confirmed to be consistent with Corrosion Under Insulation (CUI) based on the damage characteristics described in API 571. Metallographic examination revealed ferrite and pearlite phases in all samples, while the measured hardness values remained above the converted minimum hardness value of 126.4 HV for ASTM A106 Grade B carbon steel. The remaining life assessment resulted in estimated service lives of 2.0 years for the ½"-NG-01221-PC1-P6 pipe, 5.4 years for the ½"-CG-1232-MB1S-P4 pipe, and 9.2 years for the ½"-CH-02218-MB1-H2 pipe. Among the three samples, the NG pipe exhibited the most critical condition due to significant wall thinning and its shortest estimated remaining life, indicating the need for immediate inspection and maintenance to prevent premature failure. These results demonstrate that the integration of visual inspection, metallographic and SEM–EDX characterization, hardness testing, and remaining-life assessment based on API 570 and ASME B31.3 provides a practical approach for evaluating the integrity of insulated carbon steel piping in fertilizer plants. Periodic thickness monitoring and further inspection are recommended, particularly for piping with significant wall thinning, to verify the predicted remaining life and support timely maintenance decisions.

ACKNOWLEDGMENTS

The authors would like to express sincere thanks to PT. Pupuk Kalimantan Timur and the Department of Metallurgical Engineering, Universitas Pembangunan Nasional Veteran Yogyakarta for its research support.

REFERENCES

[1] W. L. Luyben, “Control structures for process piping systems,” *Chemical Engineering Research and Design*, vol. 162, pp. 28–37, Oct. 2020, doi: 10.1016/j.cherd.2020.07.022.

[2] D. G. Landtsheer, “Introduction,” in *Corrosion Under Insulation (CUI) Guidelines*, 3rd ed., UK: Elsevier Ltd, 2020, pp. 1–7.

[3] Q. Cao *et al.*, “A Review of Corrosion under Insulation: A Critical Issue in the Oil and Gas Industry,” *Metals (Basel).*, vol. 12, no. 4, p. 561, Mar. 2022, doi: 10.3390/met12040561.

[4] W. Geary, “Analysis of a corrosion under insulation failure in a carbon steel refinery hydrocarbon line,” *Case Stud. Eng. Fail. Anal.*, vol. 1, no. 4, pp. 249–256, Oct. 2013, doi: 10.1016/j.csefa.2013.09.001.

[5] S. F. Yeow, A. R. Othman, M. Mohammad, and S. B. Mohammad Agil, “Corrosion Under Insulation Probability of Failure Prediction Framework Accordance with API 581,” *International Journal of Integrated Engineering*, vol. 18, no. 2, Apr. 2026, doi: 10.30880/ijie.2026.18.02.010.

[6] M. Yang and J. Liu, “In Situ Monitoring of Corrosion under Insulation Using Electrochemical and Mass Loss Measurements,” *International Journal of Corrosion*, vol. 2022, pp. 1–12, Jan. 2022, doi: 10.1155/2022/6681008.

[7] S. Gholizadeh, “A review of non-destructive testing methods of composite materials,” *Procedia Structural Integrity*, vol. 1, pp. 50–57, 2016, doi: 10.1016/j.prostr.2016.02.008.

[8] Y. Tiandho, A. A. Tiandho, and F. Afriani, "Analisis Kuantitatif Metalografi Berdasarkan Pengolahan Citra Menggunakan Wolfram Mathematica," in *Prosiding Seminar Nasional Penelitian & Pengabdian pada Masyarakat*, 2018.

[9] Rizkivany. L., "Pengaruh Holding Time Proses Solution Treatment Dan Variasi Media Pendingin Pada Cu-Zn-Al Shape Memory Alloys Terhadap Efek Shape Memory Dan Struktur Mikro," Institut Teknologi Sepuluh November, 2020.

[10] M. A. Hendrawan and F. Yanto, "Studi Pengaruh Kekasaran Permukaan Pada Material Baja Karbon Rendah Terhadap Kekuatan Sambungan Hasil Las Titik," *Media Mesin: Majalah Teknik Mesin*, vol. 16, no. 2, Jan. 2015, doi: 10.23917/mesin.v16i2.1525.